

# Dynamic Viscoelastic Behavior of Concentrated Polymer Solutions. (I)

## Results of Some Preliminary Tests and Comparison of Dynamic and Steady Shear Data

Tadao KOTAKA and Kunihiro OSAKI\*

(Inagaki Laboratory)

Received September 27, 1961

Brief description of the parallel disk rheogoniometer was given, especially, in the case used for dynamic complex viscosity measurements. Results of certain preliminary tests for dynamic measurements gave an assurance of the reliability of the dynamic data obtained with this instruments. Dynamic data were compared with steady shear data, in which dynamic viscosity,  $\eta'(\omega)$ , and rigidity,  $G'(\omega)$ , were compared respectively with steady shear viscosity,  $\eta'(\omega)$  and normal stress,  $1/2(\sigma_{11}-\sigma_{22})$ , in toluene solutions of polystyrene. The results were in agreement with our predictions.

### INTRODUCTION

A new instrument temporarily named the parallel disk rheogoniometer<sup>1)</sup> was established for the purpose of studying viscoelastic behaviors of concentrated polymer solutions. With this instrument we had studied the non-Newtonian flow and normal stress phenomena in certain polymer-diluent systems. From these we determined two rheological parameters of flowing viscoelastic fluid, *i.e.*, the reciprocal of steady shear compliance and the steady shear viscosity, and discussed about the nature of the concomitant viscous and elastic response of the fluid.<sup>2,3,4,5)</sup>

In succession to them we have made a study of dynamic complex viscosities of polymer solutions, especially relating them to steady flow behavior. Its results will be reported here. In the next chapter we will give a brief description of the instrument and also an outline of the principle and procedures of dynamic complex viscosity measurements. Explanations for the procedures of normal and shear stress measurements were already given in our previous papers<sup>2,3)</sup> and they will not be recounted here. In the third chapter we will show results of certain preliminary tests for the validity of dynamic data obtained with this instrument. Finally in the last chapter we will show experimental results indicating the relation between dynamic data and steady flow data, *i.e.*, the relation between dynamic viscosity and steady shear viscosity and that of dynamic rigidity and normal stress data, obtained in solutions of polystyrene in toluene.

---

\*小高忠男, 尾崎邦宏

## EXPERIMENT AND PRINCIPLE

## 1. Instrument and Material

The parallel disk rheogoniometer used in the present study is shown in Fig.1. This instrument has four different functions, namely, as a parallel disk type apparatus for normal stress measurements, a rotational viscometer for steady shear viscosity measurements, an oscillatory rheometer of coaxial cylinder type and an oscillatory-rotational rheometer for studying viscoelastic response to sinusoidally oscillating shear superimposed on a continuous laminar shearing motion.



Fig. 1. The view of the parallel disk rheogoniometer. Now it is used as a rotational viscometer. This assembly can be used also for dynamic viscosity measurement.

The instrument, as is seen in Fig. 2, furnishes two sets of driving devices, the one for rotational motion and the other for oscillatory motion, each one consisting of a 1/2h.p. induction motor, a gear box of ring-cone type (gear ratio 1:4) and an eight step gear box of a planetary gear system (gear ratio 1:3 per step).

These two devices are connected through a superimposer and can give either one or both of rotational and oscillatory motion within ranges of speeds from  $1.24 \times 10^{-3}$  to 10 revolutions per second and of frequencies from  $4.5 \times 10^{-3}$  to 30 cycles per second, respectively, to the driving shaft of the main assembly. On the driving shaft either an outer disk for normal stress measurements or an outer cylindrical cup for shear stress (viscosity) measurements can be mounted. The outer container (disk or cup) is enclosed with a jacket in which thermostated oil is circulated from an oil bath, and by which temperature can be controlled at any temperature in a range from room temperature up to about  $100^{\circ}\text{C}$  within an accuracy of  $\pm 0.2^{\circ}\text{C}$ .

In the case of dynamic measurements, the cylindrical cup and bob assembly is used. That is, into the cup containing a test solution is immersed concentrically

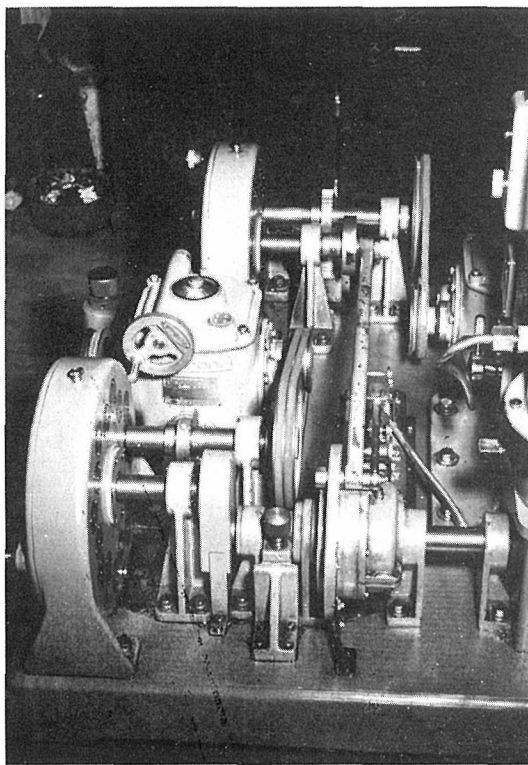


Fig. 2. The driving systems of the parallel disk rheogoniometer.

an inner cylinder (bob), which is suspended with a torsion wire. The upper end of the wire is attached to a saddle, which can be moved along a vertical slide by means of a lead screw.

A forced (oscillatory) motion of the outer cup is detected with the aid of a differential transformer which is attached to the lever connecting the deriving device and the superimposer. A response of the inner bob to this motion can be detected with a pair of differential transformers attached to the upper end of the inner bob. The output voltages generated in differential transformer circuits at the outer and inner cylinders are fed respectively to horizontal and vertical plates of a cathode-ray tube to obtain a Lissajous ellipsoid on its screen.

Materials used in this study were a commercial castor-oil (chemically pure grade) and a commercial silicone oil (Shinetsu Chem. Ind. KF 96H) for certain preliminary tests and toluence solutions of polystyrene samples  $S_1$  ( $M_w=18.2 \times 10^5$ ,  $M_n=6.43 \times 10^5$ ),  $S_3$  ( $M_w=7.26 \times 10^5$ ,  $M_n=3.96 \times 10^5$ ) and  $Th_1$  ( $M_w=15.3 \times 10^5$ ,  $M_n=7.90 \times 10^5$ ).

## 2. Principle

A rigorous solution for the motion of a viscoelastic fluid in an annular space between walls of two coaxial cylinders, in which the outer cylinder is oscillated with certain predetermined amplitude and frequency, was first given by Markovitz<sup>6)</sup> under the assumptions that the end effect of both cylinders can be neglected and the complex viscosity of the fluid is independent of the amplitude of oscillatory motion. The solution is written as:

$$1 - \frac{1}{p} (\cos\varphi + i\sin\varphi) + \sum_{n=1}^{\infty} \left( \frac{ip\omega}{\eta^*} \right)^n \left[ \frac{1}{\rho} (I-k/\omega) A_n + B_n \right] = 0,$$

where notations of the symbols are as follows :

- $p$  = amplitude ratio of bob and cup,  
 $\varphi$  = phase difference between bob and cup,  
 $\eta^* = \eta' - (iG'/\omega)$  = complex dynamic viscosity,  
 $G'$  = dynamic rigidity,  
 $\rho$  = density of the test solution,  
 $\omega$  = angular frequency ( $=2\pi\nu$ ),  
 $\nu$  = frequency in cycles per second,  
 $I$  = moment of inertia of the inner cylinder assembly,  
 $k$  = torsional constant of suspending wire.  
 $A_n$ 's and  $B_n$ 's = geometrical constants of the instrument,  
 and  $i = \sqrt{-1}$ .

Thus, when  $p$  and  $\varphi$  are determined under various known frequencies,  $\omega$ , of the outer cup, the complex dynamic rigidity,  $G'$ , can be determined as functions of frequency,  $\omega$ , by solving Eq.(1) with knowledge of instrumental constants.

It is noted that by a proper choice of dimensions of the instrument and of the frequency range investigated we may neglect the third and higher terms in the above expansion formula with respect to  $(ip\omega/\eta^*)$ . Geometrical constants for the first two terms are given as:

$$A_1 = \frac{1}{4\pi L} \frac{R_2^2 - R_1^2}{R_1^2 R_2^2}, \quad B_1 = \frac{(R_2^2 - R_1^2)^2}{8R_2^2}, \quad (2a,b)$$

$$A_2 = \frac{1}{32\pi L} \left( 4 \ln \frac{R_1}{R_2} + \frac{R_2^2}{R_1^2} - \frac{R_1^2}{R_2^2} \right), \quad (2c)$$

$$B_2 = \left\{ (R_2^2 - R_1^2)(R_2^4 - 5R_2^2 R_1^2 - 2R_1^2) + 12R_2^2 R_1^2 \ln \frac{R_2}{R_1} \right\}, \quad (2d)$$

where  $R_1$  and  $R_2$  are radii of the inner and the outer cylinder, respectively, and  $L$  is length of the inner cylinder immersed in the test fluid.

An amplitude ratio,  $p$ , and phase difference,  $\varphi$ , of two cylinders can be determined from a Lissajous ellipsoid and its circumscribed rectangle with latera parallel to the horizontal and vertical axis of the oscilloscope at each frequency of oscillation,  $\omega$ ; that is,  $p$  can be given by a ratio of two latera of the rectangle, and  $\varphi$  can be given by the use of the relation:

$$|\sin\varphi| = 4(A)/\pi[A],$$

in which  $(A)$  and  $[A]$  are area of the ellipsoid and of the rectangle, respectively. In this way, with observation of Lissajous pattern at various frequencies both components of the dynamic complex viscosity can be determined as functions of angular frequency,  $\omega$ .

## PRELIMINARY TEST FOR DYNAMIC COMPLEX VISCOSITY MEASUREMENTS

### 1. Determination of Instrumental Constants

Prior to use Eq. (1) for the determination of dynamic complex viscosities of

test solutions, it is necessary to determine instrumental constants such as  $A_n$ 's  $B_n$ 's,  $I$  and  $k$ . Among them, geometrical constants,  $A_n$ 's and  $B_n$ 's, can be readily calculated by the use of Eqs. (2a)–(2d). Since our instrument has the dimensions of  $R_1=19.0\text{mm}$ ,  $R_2=20.0\text{mm}$  and  $L=150\text{mm}$ , geometrical constants are as follows:

$$\begin{aligned} A_1 &= 1.432 \times 10^{-4}, & A_2 &= 2.39 \times 10^{-7}, \\ B_1 &= 4.75 \times 10^{-3}, & B_2 &= 2.80 \times 10^{-6} \end{aligned}$$

Terms with indices higher than  $n=3$  are all neglected.

The moment of inertia of the inner cylinder assembly,  $I$ , including the pair of cores of differential transformers attached to the inner cylinder is determined by observing a frequency  $\nu'$  for free oscillation in case of suspending by a torsion wire of known constant,  $k$ , and by the use of well known relation:  $\nu = (1/2\pi)(k/I)^{1/2}$ . For the wire of  $k=1.615$  dyne-cm/rad the observed value of  $\nu$  was  $1.111 \text{ sec}^{-1}$ , therefore the moment of inertia around the wire axis was calculated as  $I=3.314 \times 10^3 \text{ g-cm}^2$ . The above test was performed without applying an exciting current to the solenoidal coils of differential transformers. In case of the exciting current being applied to the solenoids (as in the state of measurements being performed) it was recognized that the frequency of free oscillation was increased to  $\nu'=1.124 \text{ sec}^{-1}$  for the same torsion wire. This increase in  $\nu$  may be attributed to the influence of restoring force acting on the cores due to their interaction to the magnetic field of the solenoids. Therefore, taking this influence into consideration, we used effective wire constants,  $k^*$ , defined as  $k^*=k+\Delta k$  with  $\Delta k=(2\pi)^2 I (\nu'^2-\nu^2)=3.6 \times 10^3$  instead of  $k$  for all the wires used in this study.\* The real wire constants,  $k'$ , of the torsion wires used are  $1.578 \times 10^5$  (dyne-cm/rad) for the most rigid one and  $1.015 \times 10^5$  (dyne-cm/rad) for the least rigid one.

## 2. Test with Purely Viscous (Newtonian) Fluids

It should be noted here the equation (1) was derived under the two basic assumptions: the neglect of end effect and the independence of complex viscosity on the amplitude of oscillation.

An experimental check for the validity of the former assumption and for the appropriateness of other experimental conditions can be given by the test with a purely viscous (Newtonian) fluid of known viscosity. Since the imaginary part of the complex viscosity should be zero for a purely viscous fluid, the following relations are readily derived from Eq. (1) with neglecting all the terms higher than  $n=3$ :

$$\frac{2\pi(A_1I+B_1\rho)\nu^2}{\eta'} - \frac{A_1k}{2\pi\eta'} = \frac{\nu\sin\varphi}{p} \quad (3a)$$

$$\frac{4\pi^2(A_2I+B_2\rho)\rho\nu^2}{(\eta')^2} - \frac{A_2k\rho}{(\eta')^2} = 1 - \frac{\cos\varphi}{p} \quad (3b)$$

Considering that in purely viscous fluid the real part of complex viscosity is independent of frequency and equals to the steady shear viscosity, we can expect that plots of  $(\nu/p) \sin \varphi$  and  $1-(1/p) \cos \varphi$  versus  $\nu^2$  should give straight lines

\* It was recognized that  $\Delta k$  was independent of amplitude and frequency as far as the displacement of the cores was not so large.

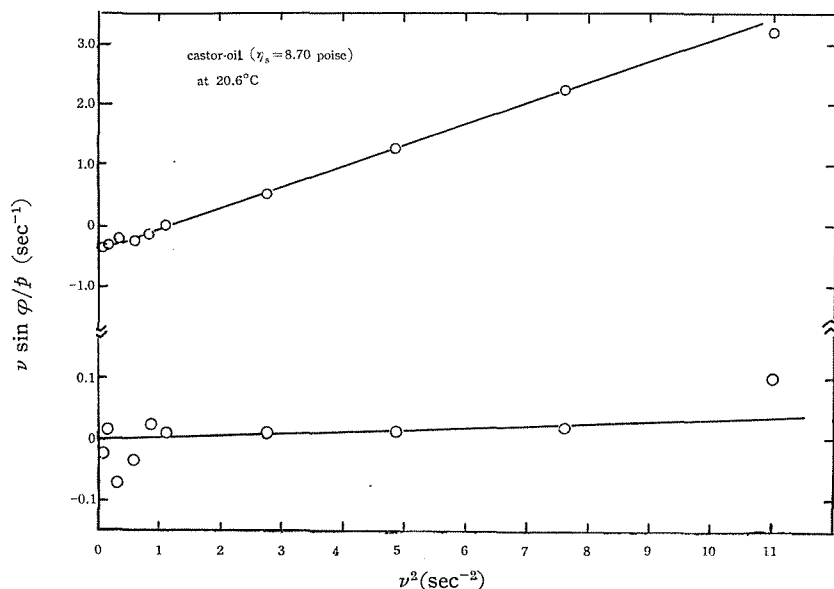


Fig. 3. Plots of  $\nu \sin \varphi/p$  and  $1-\cos \varphi/p$  versus  $\nu^2$  in a castor oil ( $\eta_s=8.70$  poise) at  $20.6^\circ\text{C}$ . Circles indicate the obtained data, and lines are calculated by Eqs. (3a) and (3b).

$$\nu \sin \varphi/p = 0.347 \nu^2 - 0.423; \quad 1 - \cos \varphi/p = 3.73 \times 10^{-3} \nu^2 - 0.512 \times 10^{-3}$$

and their slopes and intersects could be calculated from Eqs. (3a) and (3b). Such tests were performed with a castor-oil ( $\eta_s=8.70$  poise) at  $20^\circ\text{C}$  and a silicone oil ( $\eta_s=1.22 \times 10^3$  poise) at  $30^\circ\text{C}$  ( $\eta_s$  is steady shear viscosity). The former results are shown in Fig.3, in which circles are experimental values and straight lines are calculated ones from Eqs. (3a) and (3b). It is seen that the coincidence between calculated and experimental values is fairly good in the plots of  $(\nu/p) \sin \varphi$  versus  $\nu^2$ . While in the plots of  $1-(1/p) \cos \varphi$  versus  $\nu^2$  the experimental values are scattered especially at the both ends of frequency range covered with the wire used in this experimental run. However, when another wire of a different constant is used for the test, the coincidence becomes considerably good in the frequency range where the previous data are scattered.

It may be said that each wire has its most suitable range of frequency (which is rather narrow in this instrument) and beyond both ends of this frequency range the scattering of data are almost inevitable. Therefore, to cover a wide range of frequency in performing measurements we should prepare many torsion wires with widely varied torsional constants. This difficulty can be avoided also by the change of moment of inertia of the inner cylinder assembly, for instance, by attaching an inertia ring. However, as the moment of inertia of our instrument is originally considerably large, this method seems to be impractical for our instrument.

### 3. Test for Linearity

Another test which should be made before performing the measurements is to find the frequency range in which the linearity assumption holds valid. That is,

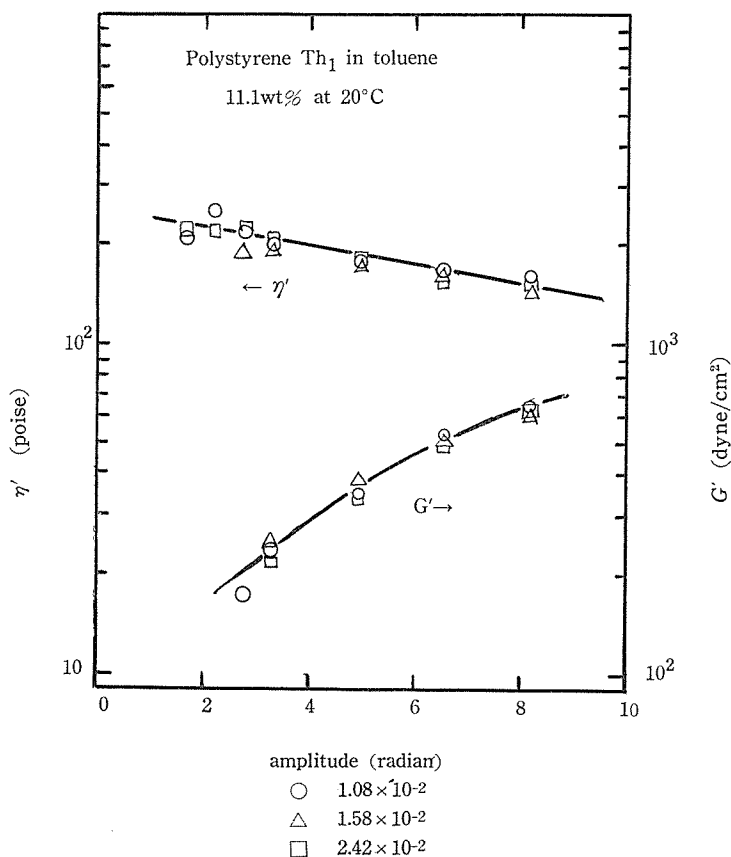


Fig. 4. Test for the dependences of dynamic viscosity and dynamic rigidity,  $G'$ , on the amplitudes of the outer cylinder: 11.1wt% polystyrene Th<sub>1</sub> in toluene at 20°C

in deriving Eq. (1) the complex viscosity of the fluid is assumed to be independent of the amplitude of the oscillatory motion of the outer cylinder. This limit in the amplitude may depend on dimension of the instruments as well as the rheological nature of the material to be tested. In our experiment this test was made by comparing the  $G'$  and  $\eta'$  values measured in polystyrene-toluene solutions at three different amplitudes,  $1.08 \times 10^{-2}$ ,  $1.58 \times 10^{-2}$  and  $2.42 \times 10^{-2}$  radian, in the range available with this instrument.

A result for a 10% solution of polystyrene Th<sub>1</sub> in toluene at 20°C is shown in Fig. 4. It is seen that the coincidence of  $G'$  and  $\eta'$  values obtained at different amplitudes is considerably good in the frequency range investigated. Thus in this experiment we use the amplitude range from  $1.0 \times 10^{-2}$  to  $1.5 \times 10^{-2}$  radian for all the solutions investigated.

#### COMPARISON OF DYNAMIC DATA WITH STEADY SHEAR DATA

The relation between dynamic and steady shear viscosities has been discussed hitherto by various authors from both theoretical and experimental points of

view. Theoretical treatment by DeWitt<sup>7)</sup> predicted that the steady shear viscosity as a function of rate of shear should be the same as the dynamic viscosity as a function of angular frequency. Experimental check of this prediction by various authors,<sup>8,9,10)</sup> however, showed that both the viscosities were coincident with each other only at low frequencies, and the dynamic viscosity decreased more rapidly than did the steady shear viscosity. Our results, as is seen in Figs. 5a and 5b, also show this discrepancy, which suggests that the rate of shear dependence of steady shear viscosity is not quite quantitatively equivalent to the angular frequency dependence of dynamic viscosity.

The relation between dynamic rigidity and normal stresses was discussed by Markovitz and Williamson,<sup>11)</sup> who proposed that if  $1/3(\sigma_{11}-\sigma_{22})=f(\dot{\epsilon})$ , then  $G'(\omega)=f(1.4\omega)$ , in which  $\sigma_{11}$  and  $\sigma_{22}$  denote components of normal stress in the direction of flow and in the direction perpendicular to the plane of shear, respectively, and  $\dot{\epsilon}$  denotes the rate of shear. The factor of 1.4 was obtained empirically. Our analysis on the basis of a simple molecular theory<sup>4,12)</sup> suggests, however, that the angular frequency dependence of dynamic viscosity tends to the same form to the rate of shear dependence of  $1/2(\sigma_{11}-\sigma_{22})$  when the rate of shear and angular frequency approach zero. For the relation between dynamic and steady shear viscosities, the analysis predicts that both viscosities tend to the same value at very small frequencies, and in both cases the steady shear data,  $1/2(\sigma_{11}-\sigma_{22})$  and

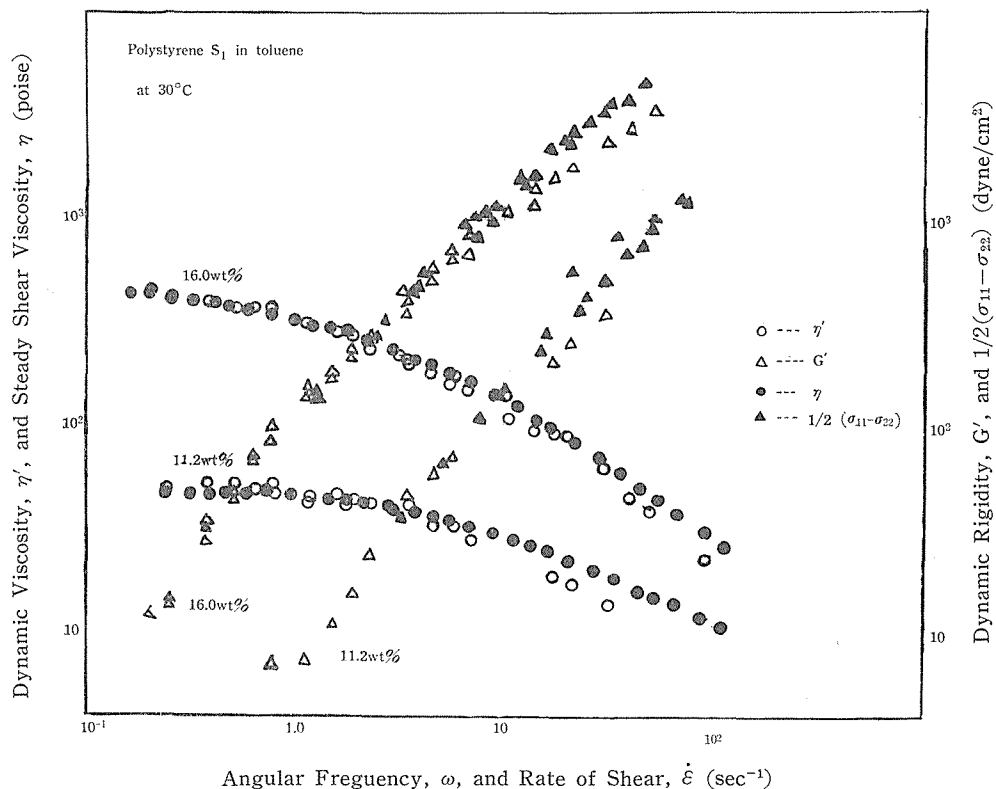


Fig. 5a. Comparison of dynamic data with steady shear data: polystyrene  $S_1$  in toluene at 30°C.



Viscoelastic Behavior of Polymer Solutions

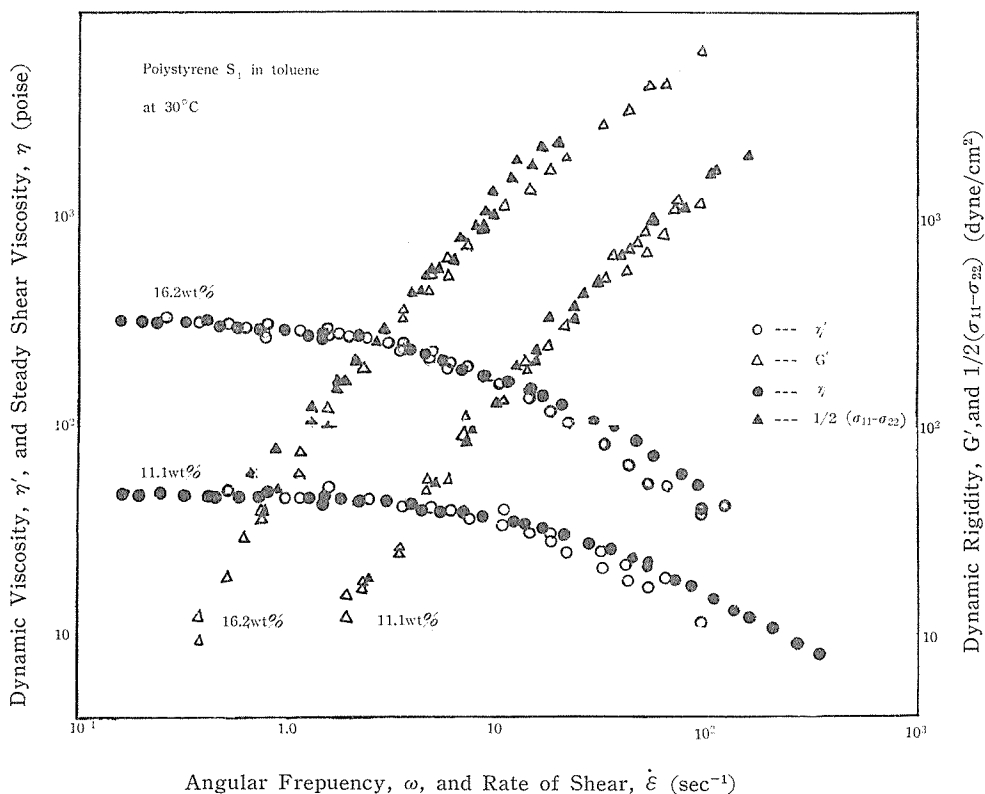


Fig. 5b. Comparison of dynamic data with steady shear data: polystyrene  $Th_1$  in toluene at  $30^\circ\text{C}$ .

$\eta(\dot{\epsilon})$ , are always larger than the corresponding dynamic data  $G'(\omega)$  and  $\eta'(\omega)$  at finite value of  $\dot{\epsilon}$  or  $\omega$ . On this standpoint we compared  $1/2(\sigma_{11}-\sigma_{22})$  with  $G'(\omega)$ , indentifying the rate of shear,  $\dot{\epsilon}$ , with the angular frequency,  $\omega$ .

The results are shown in Figs. 5a and 5b for toluene solutions of polystyrene  $S_1$  and  $Th_1$  obtained at  $30^\circ\text{C}$ . It is seen that both of normal stress and dynamic rigidity curves coincide with each other fairly well at low frequencies, and again slight discrepancies are recognized between both curves, that is, the former increases more rapidly than does the latter. These results are, at least, in qualitative agreement with the theory outlined above. However, it seems that this agreement is somewhat fortuitous, since the theories were derived for very dilute solutions with a simple molecular model. Theoretical consideration from more general standpoint is necessary to determine whether the above comparison has a general applicability, especially, whether the factor of 1/2 for normal stress data is a universal constant or only a factor applicable for some limited cases.

The authors are indebted to Professors Hiroshi Inagaki and Mikio Tamura for their interests in this work. One of the authors (TK) expresses his thanks to the Japan Society for the Promotion of Science for a Postdoctoral Fellowship Grant (Oct., 1960—March, 1961) which enabled him to participate in this work.

**REFERENCES**

- (1) M. Tamura, M. Kurata and T. Kotaka, *Zairyoshiken*, **8**, 335 (1959).
- (2) M. Tamura, M. Kurata and T. Kotaka, *Bull. Chem. Soc., Japan*, **32**, 471 (1959).
- (3) T. Kotaka, M. Kurata and M. Tamura, *J. Appl. Phys.*, **30**, 1705 (1959).
- (4) T. Kotaka, M. Kurata and S. Onogi, *Prog. Theor. Phys. Suppl.*, No. 10, 101 (1959).
- (5) T. Kotaka, M. Kurata and M. Tamura, unpublished work.
- (6) H. Markovitz, *J. Appl. Phys.*, **13**, 1070 (1952).
- (7) T.W. DeWitt, *J. Appl. Phys.*, **26**, 889 (1955).
- (8) T.W. DeWitt, H. Markovitz, F.J. Padden, Jr. and L.J. Zapas, *J. Colloid Sci.*, **10**, 174 (1955).
- (9) W. Philippoff, *J. Appl. Phys.*, **25**, 1102 (1954).
- (10) S. Onogi, I. Hamana and H. Hirai, *J. Appl. Phys.*, **29**, 1503 (1958).
- (11) H. Markovitz and R.B. Williamson, *Trans. Soc. Rheology*, **1**, 25 (1957).
- (12) S. Onogi and T. Kotaka, *Rheology of Concentrated Polymer Solutions*, in *Rheology for Chemical Engineers*, (in Japanese) ed. by S. Onogi, Makishoten, Tokyo, 1959, pp. 54-83.